

Direct investigation of localized hole states in pseudomorphic modulation-doped $\text{Al}_x\text{Ga}_{1-x}\text{As}/\text{In}_y\text{Ga}_{1-y}\text{As}/\text{GaAs}$ heterostructures by optical detection of quantum oscillations

G. G. Tarasov

*Department of Physics, Humboldt-Universität zu Berlin, Invalidenstrasse 110, D-10115 Berlin, Germany
and Institute of Semiconductor Physics, National Academy of Sciences, Prospect Nauki 45, 252650 Kiev, Ukraine*

U. Müller

Department of Physics, Humboldt-Universität zu Berlin, Invalidenstrasse 110, D-10115 Berlin, Germany

Yu. I. Mazur

*Department of Physics, Humboldt-Universität zu Berlin, Invalidenstrasse 110, D-10115 Berlin, Germany
and Institute of Semiconductor Physics, National Academy of Sciences, Prospect Nauki 45, 252650 Kiev, Ukraine*

H. Kissel

Department of Physics, Humboldt-Universität zu Berlin, Invalidenstrasse 110, D-10115 Berlin, Germany

Z. Ya. Zhuchenko

Institute of Semiconductor Physics, National Academy of Sciences, Prospect Nauki 45, 252650 Kiev, Ukraine

C. Walther and W. T. Masselink*

Department of Physics, Humboldt-Universität zu Berlin, Invalidenstrasse 110, D-10115 Berlin, Germany

(Received 4 February 1998; revised manuscript received 24 March 1998)

The valence-band structure in $\text{Al}_x\text{Ga}_{1-x}\text{As}/\text{In}_y\text{Ga}_{1-y}\text{As}/\text{GaAs}$ heterostructures ($x=0.2$, $y=0.1$) is investigated using a magnetic method for probing the electronic structure in two-dimensional (2D) heterostructures through the optical detection of quantum oscillations (ODQO). For structures with narrow $\text{In}_y\text{Ga}_{1-y}\text{As}$ quantum wells ($W < 15$ nm), the quantum oscillations with the Fermi sea reveal two distinct periods in $1/B$. This behavior is attributed to the existence of two classes of hole localization: a shallow one, primarily resulting in hole scattering, and a deep localization resulting in a 10-meV shift in the ODQO. In wider $\text{In}_y\text{Ga}_{1-y}\text{As}$ quantum wells ($W = 15$ nm), where the two-period behavior begins to disappear, excitonic luminescence is observed in addition to the 2D-electron features. This excitonic contribution strongly modifies the development of photoluminescence signature into Landau-level fan. [S0163-1829(98)04832-2]

I. INTRODUCTION

High-quality III-V semiconductor heterostructures are well suited for the study of electrons and holes confined in one spatial direction under both equilibrium and nonequilibrium conditions.¹⁻⁴ Because the conduction band, also including a quasi-two-dimensional electron gas (2DEG), is relatively well understood, data that involve both electrons and holes in a heterostructure can be used to extract information about the structural details of the valence band. These details play a decisive role when the optical and transport phenomena in quantum wells are under investigation; the valence band is especially complex in strained systems such as the modulation-doped lattice-mismatched n -type $\text{Al}_x\text{Ga}_{1-x}\text{As}/\text{In}_y\text{Ga}_{1-y}\text{As}/\text{GaAs}$ heterosystem. The physical picture is further complicated when the lattice mismatch leads to partial relaxation of the $\text{In}_y\text{Ga}_{1-y}\text{As}$ through dislocation generation. Depending on composition and the quantum well width, edge- and/or surface-propagating misfit dislocations may be generated. For both types of dislocations, the maximum thickness of the strained $\text{In}_y\text{Ga}_{1-y}\text{As}$ on the unstrained GaAs without generating dislocations is referred to as the critical layer thickness (CLT).⁵⁻⁷ Two distinct types

of photoluminescence (PL) behavior are observed: (i) a strong, single, and narrow excitonic emission from a homogeneously strained (not relaxed) $\text{In}_y\text{Ga}_{1-y}\text{As}$ QW below CLT and (ii) a broad emission attributed to impurities and interface states can develop above or near CLT.

We have recently observed a characteristically different PL in n -type $\text{Al}_x\text{Ga}_{1-x}\text{As}/\text{In}_y\text{Ga}_{1-y}\text{As}/\text{GaAs}$ heterostructures ($x=0.2$, $y=0.1$) with width just below CLT.⁸ For structures with a $\text{In}_y\text{Ga}_{1-y}\text{As}$ QW width $d = 20$ nm—only slightly narrower than the expected CLT of 25 nm for $y=0.1$ —the excitonic PL was dominant with a clearly pronounced shoulder, presumably due to the 2D electron-acceptor bound hole recombination. When the QW thickness is reduced to 12 nm, however, the PL feature transforms into broad intersubband emission.

Typically this type of emission is attributed to the recombination of high-density electrons throughout the Fermi sea with the low-density holes, which are assumed to be either sufficiently localized or can be scattered during the recombination. This latter assumption is necessary to break the momentum \mathbf{k} conservation expected for the direct band-to-band transitions. Various mechanisms could be responsible for the breakdown of this selection rule, but hole localization caused

by alloy fluctuations and/or interface defects probably plays the most important role. Experimentally one observes an enhancement of the Fermi edge singularity (FES),^{9–12} which strongly modifies the emission line shape due to nonvertical transitions between the 2D electrons at the Fermi energy and thermalized holes. The hole localization favors this process. A possible mechanism could be that the holes are bound electrostatically and then their delocalization is expected for a high-density electron gas due to screening. Experimentally, however, data that describe how the screening influences the interaction between excitons and longitudinal optical phonons indicate that the hole localization exists even in lattice-matched $\text{In}_x\text{Ga}_{1-x}\text{As-InP}$ QW,¹³ favoring a nonelectrostatic explanation for the hole localization.

Recent magneto-PL experiments¹⁴ for $\text{Al}_x\text{Ga}_{1-x}\text{As/In}_y\text{Ga}_{1-y}\text{As/GaAs}$ modulation-doped single QW's with high sheet electron density ($N_s = 2.1 \times 10^{12} \text{ cm}^{-2}$) revealed a strong enhancement of PL intensity oscillations at the Fermi energy (associated with even filling factor). The reason for these oscillations is still unclear and is assumed to be a Landau-level-exciton coupling and/or the changes in the Hartree self-consistent potential. Nevertheless, the peaks in magnetoluminescence are attributed to inter-Landau-level (N) transitions with $\Delta N \neq 0$. The violation of the selection rule ($\Delta N = 0$) is attributed to the alloy disorder potential or impurities; on the other hand, no verification of hole localization was found. Thus, the hole localization is of utmost importance for the understanding of PL behavior in quasi-two-dimensional structures and deserves a thorough investigation. In the present work, we present evidence for such localization based on a magnetoluminescence study in pseudomorphic modulation-doped $\text{Al}_x\text{Ga}_{1-x}\text{As/In}_y\text{Ga}_{1-y}\text{As/GaAs}$ heterostructures. Our results center on the optical detection of quantum oscillations via PL in magnetic field as described in Ref. 15. The localization energy is determined for specific heterostructures and found to be substantially dependent on the growth conditions.

II. EXPERIMENTAL DETAILS

The samples used in this investigation are pseudomorphic $\text{In}_y\text{Ga}_{1-y}\text{As}$ modulation-doped quantum wells grown on semi-insulating, (100)-oriented GaAs substrates in a Riber 32-P gas-source MBE (GSMBE) system. The typical epitaxial layer sequence consists of a GaAs buffer layer, an undoped $\text{In}_y\text{Ga}_{1-y}\text{As}$ strained QW (2DEG channel), an $\text{Al}_x\text{Ga}_{1-x}\text{As}$ undoped spacer, an $\text{Al}_x\text{Ga}_{1-x}\text{As}$ heavily Si-doped supplier layer, and a Si-doped GaAs cap layer. The range of $\text{Al}_x\text{Ga}_{1-x}\text{As}$ and $\text{In}_y\text{Ga}_{1-y}\text{As}$ layer compositions spreads into $0.15 \leq x \leq 0.20$ and $0.08 \leq y \leq 0.17$, respectively. Double-crystal x-ray diffraction and simulation of the double x-ray rocking curve were used to verify the samples' structural parameters. The measurements were carried out using a Bede Q1B x-ray diffractometer using the symmetric (004) reflex. The typical x-ray diffraction curve shown in Fig. 1 is also indicative of the high quality of the structures under consideration. The structural parameters of the samples determined from this study are listed in Table I together with the electron densities N_s and the dc mobility μ_{dc} of the 2D electrons, obtained from the low-field Hall measurements down to 4.2 K. The PL was excited by the 514.5-nm line of

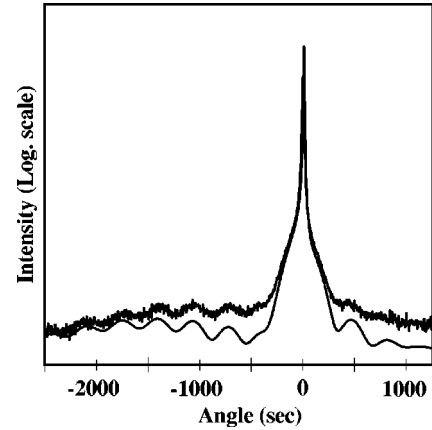


FIG. 1. The x-ray rocking curve for the $\text{Al}_x\text{Ga}_{1-x}\text{As/In}_y\text{Ga}_{1-y}\text{As/GaAs}$ ($x=0.2$, $y=0.1$) PHEMT structure (upper curve) and the result of simulation (lower curve).

a cw Ar^+ laser and the excitation densities were in the range of 50 mW/cm^2 to 20 W/cm^2 . The PL signal was dispersed through a 3/4-m Czerny-Turner scanning spectrometer, with a spectral resolution better than 0.1 meV , and detected using phase-sensitive detection with a thermoelectrically cooled photomultiplier tube [containing a GaAs(Cs) photocathode] or a LN_2 cooled high-purity Ge detector. The samples were mounted in an Oxford Spectromag 4000 system, which allows measurements in magnetic fields up to 7 T and at temperatures from 1.7 to 300 K.

III. RESULTS AND DISCUSSION

In what follows we focus on the optical properties of n -type pseudomorphic modulation-doped QW heterostructures similar to those used in high-electron-mobility transistors (PHEMT). The emission is dominated by a broad band, predominantly resulting from the recombination of 2D electrons with heavy holes. For the In content and the QW

TABLE I. Structural and electronic parameters of the two samples studied.

Samples		1	2
GaAs:Si (cap layer)	$d(\text{nm})$	5	5
	$N_D(10^{18}\text{cm}^{-3})$	2.5	2.5
$\text{Al}_x\text{Ga}_{1-x}\text{As:Si}$ (supplier layer)	$d(\text{nm})$	35	35
	x	0.20	0.20
	$N_D(10^{18}\text{cm}^{-3})$	2.0	2.0
$\text{Al}_x\text{Ga}_{1-x}\text{As}$ (spacer layer)	$d(\text{nm})$	8	7.5
	x	0.20	0.20
$\text{In}_y\text{Ga}_{1-y}\text{As}$ (quantum well)	$D(\text{nm})$	12	15
	y	0.10	0.10
GaAs (buffer layer)	$d(\text{nm})$	200	500
Hall data (at 12 K):			
	$N_s(10^{11}\text{cm}^{-2})$	6.3	2.5
	$\mu_{dc}[10^3\text{cm}^2/(\text{V s})]$	40	3

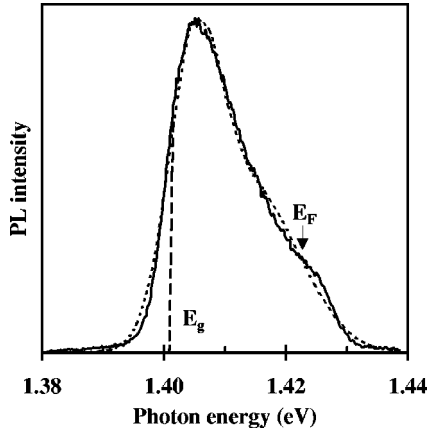


FIG. 2. PL spectrum for sample 1 without magnetic field at $T = 6$ K. The dashed line is a fit using Eq. (1).

widths used in this study ($0.1 \leq y \leq 0.15$ and $d \sim 10 - 15$ nm) the strain relaxation caused by the dislocation generation is essentially absent⁵ and therefore the confined heavy holes ($j_z = \pm 3/2$) are the only holes that will be taken into consideration in the analysis of our data. Figure 2 shows the low-temperature PL spectrum for sample 1. The overall width of the PL feature without magnetic field at $T = 4.2$ K is about 33 meV when measured from the low-energy side of the luminescence to the Fermi energy. The Fermi energy is derived from the sheet density N_s of the 2DEG, using the relation $(E_F - E_{e1}) = \pi \hbar^2 N_s / m_e^*$ for cases with only one occupied subband. Taking the measured N_s for sample 1 equal to $N_s = 6.3 \times 10^{11} \text{ cm}^{-2}$ (see Table I) and the electron effective mass in a strained-layer $\text{In}_y\text{Ga}_{1-y}\text{As}$ QW with $y \approx 0.1$ equal to 0.068 the Fermi energy is found to be 23 meV above the lowest electron subband. The PL signature width exceeds this value by approximately 10 meV. The PL feature demonstrates clearly the short-wavelength cutoff, indicating the position of the Fermi edge. The line shape observed is typical for a QW with comparatively low disorder and a high density of free carriers. In this case the electron-hole recombination is completely allowed only for vertical transitions close to $k = 0$. Being increasingly more strongly forbidden due to the requirements of wave-vector conservation, the allowed transitions decrease in intensity toward $k_F \approx 2 \times 10^6 \text{ cm}^{-1}$, the situation clearly seen in Fig. 2. The presence of hole localization in real space introduces the larger Fourier components of the order of k_F into a hole wave function, resulting in an increase of recombination at k_F ; this is not the case shown in Fig. 2. Thus the PL feature shape here is consistent with weak hole localization and/or comparatively low disorder.

The analysis has been performed in more detail in terms of a theory developed by Lyo and Jones for the PL line shape in modulation-doped QW structures.¹⁶ In the low-temperature limit and for low-intensity cw excitation, the line shape is described by the function S_{ij} ,

$$S_{ij}(\varepsilon) \propto \int_0^\omega f(\tau - \mu_{vj}) f(\varepsilon - \tau - \mu_{ci}) K(\omega\tau) d\tau. \quad (1)$$

Here ε is the photon energy minus the effective band gap, f is the Fermi distribution function, μ_{vj} and μ_{ci} denote the

chemical potentials for j th valence and i th conductivity bands, respectively. The Lorentzian K represents the processes including direct transitions allowed in \mathbf{k} space and indirect transitions assisted by impurities. The total linewidth arises here from the collision-induced broadening of the carrier levels, Fermi-level effects due to impurity-assisted processes, and temperature effects through the thermal distribution of the minority carriers. Following the procedure described in Ref. 16, we have found that the PL feature can be very well fit with the energy gap $E_g = 1.40$ eV. The dominant influence on the PL shape arises from the recombination of the thermalized low-energy holes and electrons with the same wave vectors. But at $T = 4$ K this contribution alone would result in luminescence, which rises very steeply above the band-gap threshold and peaks at lower energies than what is experimentally measured. When the impurity-assisted processes are included, they broaden and shift the spectral profile to the high-energy side due to subtraction of the intensity from the low-energy side and adding it to the high-energy region. Without further analysis, indirect processes shift the spectral distribution maximum too far to the high-energy side (by 12 meV) with respect to E_g . By correctly including the spacer-layer thickness d of the structure, however, an accurate fit of the experimental data is possible. The results of the fit as described above are shown in Fig. 2 by a dashed line. The low-energy tail of the PL feature is approximated by the Urbach form. Thus, the PL profile is reasonably explained in terms of ionized-impurity scattering of the majority and minority carriers.¹⁶ The electron-hole recombination is shown to be accompanied by impurity and disorder-assisted processes, which result in broadening and shifting of the PL line. In order to focus on hole-related perturbations, we augment the study with magnetoluminescence.

The magnetic field dependence of the PL is depicted in Fig. 3. In a magnetic field B , the spectrum breaks up into a series of equally spaced Landau levels (LL); the spacing corresponds exactly to the electron cyclotron energy eB/m_e^*c . These data indicate that the 2DEG states are not significantly perturbed by disorder or localizing defects because they are very well described by a simple theory of Landau quantization. Extrapolation of the curves to $B = 0$ as in Fig. 3(b) allows a precise determination of the band gap of $E_g = 1.401 \pm 0.001$ eV. At the bottom of Fig. 3(b), the LL even filling factors ($\nu = N_s h / eB$) including spin are shown by vertical bars. No electron spin splitting is observed. Electron-hole emission is expected to arise primarily from the $0 \rightarrow 0$ transition and secondarily from indirect transitions $1 \rightarrow 0$, $2 \rightarrow 0$, $3 \rightarrow 0$, etc., as assigned in Fig. 3(b).

The low-temperature peak intensities do not follow a Boltzmann distribution, being determined to a very large extent by the off-diagonal matrix elements and resulting in indirect transitions.² As the magnetic field is increased from $B = 3$ T, the successive electron LL crosses the E_F , so that at $B = 7$ T only two LL's have a significant population (filling factor $\nu = 4$). At this field, the separation between $N = 0$ and $N = 1$ LL's takes the value 11.8 meV, whereas the corresponding PL features widths are 6.8 and 5.1 meV, respectively. The widths of the electron LL's cannot be deduced directly from the widths of the observed PL peaks because the latter are determined basically by inhomoge-

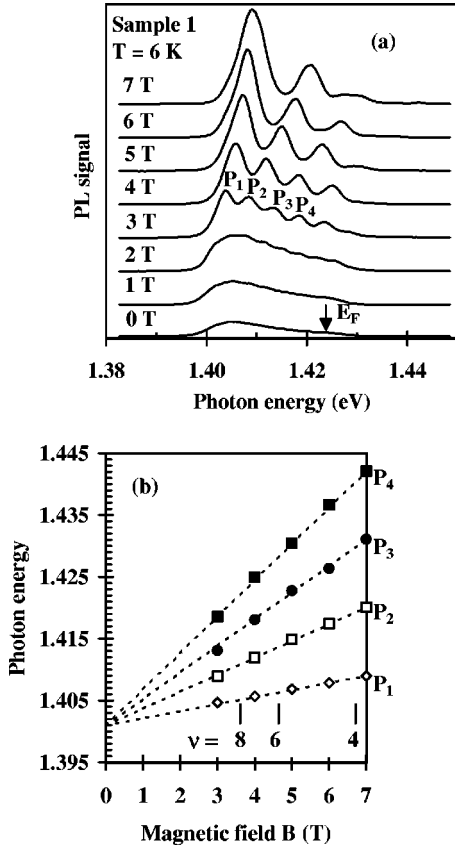


FIG. 3. PL spectrum transformation for sample 1 in magnetic fields: (a) Magnetic field assisted transformation of PL signature. (b) Landau level fan plot. P_1 corresponds to the $0 \rightarrow 0$ transitions, P_2 to $1 \rightarrow 0$, P_3 to $2 \rightarrow 0$, and P_4 to $3 \rightarrow 0$, respectively. The filling factors are shown by vertical bars.

neous processes such as the QW width and alloy fluctuations. The PL component widths (Γ) are found to be as follows: for $N=0$, $\Gamma=6.4$ meV; for $N=1$, $\Gamma=4.9$ meV; and for $N=2$, $\Gamma=3.8$ meV; consistent with broadening by long-range potential fluctuations of the order of the cyclotron radius evaluated to be 97 \AA at $B=7 \text{ T}$.

In order to investigate the relative contribution produced by the hole localization, we compare SdH and PL measurements of the same samples. The magneto-optical studies are based on optical detection of quantum oscillations (ODQO) in a continuously varied (swept) magnetic field. Similar oscillatory behavior of the PL intensity at the Fermi energy has been widely used in investigations of the 2D conduction-band behavior.^{17–19} The behavior is associated with the interaction between the optically excited hole and the electron of the 2DEG at the Fermi energy. The Fermi level of a 2DEG system is pinned at the highest occupied LL in magnetic field. When the field is swept up, the density of states per LL increases. Since the electron concentration remains essentially constant, the LL's become depopulated as the magnetic field increases. Each time a LL is totally emptied, the Fermi level moves to the next successively lower LL. This description pertains to the even filling factor ν . If, on the other hand, the observation energy (the monitor position E_m) is kept fixed (similarly to the PL excitation spectra measurement) and the magnetic field scanned, the PL intensity is expected to become enhanced whenever the selected energy

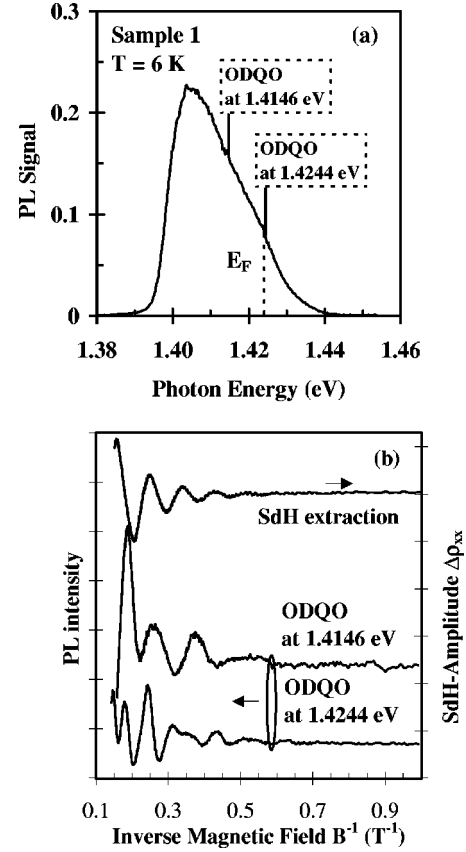


FIG. 4. ODQO data obtained at different energies within the PL spectrum from sample 1: (a) Monitor positions within the PL spectrum. (b) The PL intensity minus a constant offset shows the ODQO patterns for selected monitor positions. SdH data are also plotted for comparison.

position coincides with the LL energy. In this case, it is possible to independently study the filling of different quantum subbands by monitoring the corresponding PL transitions. This new technique was successfully applied to the study of the Si-modulation-doped InP/In_yGa_{1-y}As/InP QW and InP/In_yGa_{1-y}As heterostructures.¹⁵ Following the technique described in Ref. 15, we have used this sensitive method of optical detection of quantum oscillations complementary to SdH and magneto-luminescence in n -type Al_xGa_{1-x}As/In_yGa_{1-y}As/GaAs PHEMT structures in order to explore the valence band.

The 2D electron-hole recombination in a magnetic field results in emission at

$$E_m = E_g + \left(N + \frac{1}{2}\right) \frac{eB}{m_e^*} = E_g + \left(N + \frac{1}{2}\right) \hbar \omega_c. \quad (2)$$

Here E_g is the energy separation between the lowest electron and hole subbands.

The PL intensity oscillates with respect to the inverse magnetic field with period

$$\Delta\left(\frac{1}{B}\right)_{\text{ODQO}} = \left(\frac{m_e^*(E_m - E_g)}{\hbar e}\right)^{-1}. \quad (3)$$

Equations (2) and (3), following Ref. 15, are used for determination of E_g and sheet density N_s . Figure 4(a) shows the

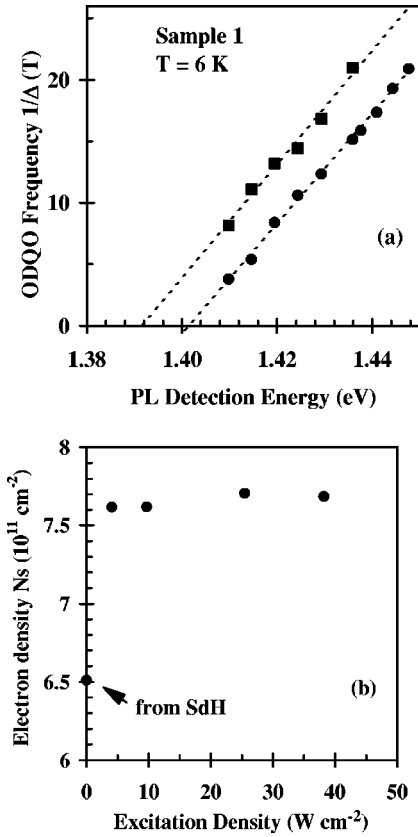


FIG. 5. (a) The dependence of the inverse ODQO period on the monitor position within the PL feature, as extracted from dI_{PL}/dB ; the data are also resolved in the raw data as plotted in Fig. 4(b). (b) Nonequilibrium 2DEG density in sample 1 vs the excitation density. The point on the vertical axis was derived from SdH measurements.

PL spectrum of sample 1 at $T=6$ K and two monitor energies within the E_g and E_g+E_F spacing scanned by magnetic field. Quantum oscillation patterns are shown in Fig. 4(b) for luminescence at the two monitored energies. The oscillations are clearly observed at comparatively low magnetic fields (down to 1.5 T), whereas the LL splitting is detectable in magnetic fields as small as 3 T (see Fig. 3). Oscillations weaker than those depicted in Fig. 4(b) were resolved by measuring dI_{PL}/dB ; by measuring the derivative, the inverse period can be extracted even with weak oscillations. When the PL is monitored near E_F , the shape of ODQO is remarkably similar to that of the SdH oscillations [Fig. 4(b)] measured in the same samples. The total concentration of 2D electrons was derived from the relation

$$N_s = \frac{2e}{\hbar} \left[\Delta \left(\frac{1}{B} \right) \right]_{ODQO}^{-1} \quad (4)$$

due to coincidence of the ODQO period and the period of SdH oscillations: $\Delta(1/B)_{ODQO} = \Delta(1/B)_{SdH}$. From these data, N_s was calculated to be $N_s = 6.51 \times 10^{11} \text{ cm}^{-2}$. The inverse ODQO period is a linear function of the monitor position E_m [see Eq. (3)]. Figure 5(a) depicts the experimental dependence Δ^{-1} (points) on E_m . Two sets of data can easily be distinguished. The lower one is well approximated by the straight line, which crosses the energy axis at $E_m = E_g$

$= 1.401 \pm 0.001$ eV, thereby coinciding exactly with the E_g value determined above. The upper set of data points also falls onto a single straight line, which crosses the abscissa at E_m , shifted by approximately 10 meV with respect to E_g . We believe that such behavior of ODQO reflects the existence of localized hole states within the energy gap. The localization energy can under this assumption be derived from Fig. 5(a) and equals $\Delta E_{loc} = 10$ meV.

A given energy selects two states within the energy bands for which the emission of light quanta are possible. If this energy is fixed to a filled LL of 2D electrons whose energy shifts with magnetic field, the measured luminescence peaks each time the successive energy states of the valence band are approached. Some of them are located near the top of the valence band and describe the holes with small localization energy and are most strongly scattered by large inhomogeneities and potential fluctuations. These holes primarily determine the energy gap and are responsible for the lower set of data plotted in Fig. 5(a). The other holes are trapped at a deeper energy. This characteristic depth is determined by alloy fluctuations and has the value about of 10 meV in the structure described here. Both of the states described above are allowed to be populated at low temperature.

For energies within the interval $E_g < E < E_g + E_F - E_{loc}$, we observe two ODQO periods because the localized hole state can be reached when the selected LL is still filled. For larger energies $E > E_g + E_F - E_{loc}$, however, there is only one ODQO period due to fact that the LL is empty when the localized hole state is approaching. This behavior is clearly seen in Fig. 5(a). The second period is not detectable starting from $E_g = 1.435$ meV. A more complicated situation should be expected in the close vicinity of E_g and below it, when the Urbach tail is involved. In this case, we observe the ODQO strongly broadened and an additional period seems to arise. The nature of this state detected by means of ODQO is not yet clear.

Our data are in general agreement with the results of several other optical investigations of $\text{In}_y\text{Ga}_{1-y}\text{As}$ QW's both in strained and in lattice-matched structures. Skolnick *et al.*¹³ for example deduced the hole localization in doped $\text{In}_y\text{Ga}_{1-y}\text{As-InP}$ QW's from Stokes shift of 12 ± 3 meV, comparing the PL and photoconductivity data. Similar results were also obtained for undoped QW's.²⁰ Calculations have shown that the likely hole-binding potential persists at high N_s . The 2D electron gas was shown to give poor screening at the length scale of hole-binding potential ($< 80 \text{ \AA}$). The hole localization in Ref. 13 is assumed to arise either from well width fluctuations or from the microscopic fluctuation in alloy composition. Evidence for alloy fluctuations (so-called "spinodal decomposition") on the 10-20-nm scale has been found in thick layers of $\text{In}_y\text{Ga}_{1-y}\text{As}$.²¹ A further support for the idea of alloy fluctuations being responsible for the hole localization is due to Andersson *et al.*⁵ where it was shown that high-quality strained single and multiple QW structures can be grown only provided the thickness of the strained layers is kept small enough (less than CLT) to avoid misfit dislocation generation. This CLT was found to be approximately inversely proportional to In content. Even in these high-quality structures, however, a low-energy tail of PL was related to the emission of exciton bound to impurity centers in the QW or localized at potential

minima due to inhomogeneities in the In concentration. Studying the localization effects, energy relaxation, and the electron and hole dispersion in selectively doped n -type $\text{Al}_x\text{Ga}_{1-x}\text{As}/\text{In}_y\text{Ga}_{1-y}\text{As}/\text{GaAs}$ quantum wells⁶ it was concluded that at low temperatures and at low excitation intensities, the thermal distribution of holes does not provide enough free holes with sufficient momentum to allow direct transitions of the Fermi electrons. In order to provide the large emission recombination of Fermi electrons, the holes have to be localized due to spatial fluctuations of the valence-band edge, which is of the order of k_F^{-1} . The results cited above provide further support to our hypothesis regarding the interpretation of ODQO study in the HEMT structures in terms of hole localization.

An important question is to what extent the two sorts of localized holes observed by means of ODQO can also be observed in the data of Fig. 2 and/or in the plot of PL peak positions versus magnetic field in Fig. 3(b). The description of the PL line shape (of Fig. 2) without magnetic field does not take into consideration a more strongly localized hole state as is observed in the ODQO data of Fig. 5(a), but fits the luminescence data quite well. A more careful examination of Fig. 2, however, reveals that in the vicinity of E_F , the fit is not especially good. Although fairly weak, an enhanced PL signal near E_F is clearly evident, similar to data reported in similar systems.^{16,22,23} The same majority of hole states is responsible for the nominally forbidden $N_e - N_h = 1, 2, 3$ (N_e and N_h label LL for the electron and hole, respectively) transitions seen in Fig. 3. Being determined by the weak hole perturbation the Landau level fan plot [Fig. 3(b)] converges to a single point, E_g . A LL series related to the strongly localized hole cannot be seen here because it is far too weak, as in the $B=0$ T case.

The ODQO technique, on the other hand, offers a higher sensitivity in comparison with a conventional magneto-optical spectroscopy and allows detection and extraction of the low-density excitations even when they are hidden in the other signal. Figure 4(b) depicts the measured PL intensity (I_{PL}) (minus a constant offset) versus inverse magnetic field. Even more sensitivity is obtained when the derivative dI_{PL}/dB is detected experimentally and analyzed. In this case, the small variations of I_{PL} are transformed into large changes of derivative and the period can be measured even in weak signals.¹⁵ The oscillation frequencies of these sets of data are determined using the derivative of the luminescence data and plotted in Fig. 5(a). [The points obtained from the data presented in Fig. 4(b) can also be extracted directly from the raw data without the necessity of differentiation.] As one clearly sees, two types of hole localization are accurately measured by means of ODQO, while the strongly localized holes of low density are observed only weakly and indirectly in PL and in the magneto-optical investigations. There is, however, no contradiction between these two presentations of the data, but only a realization that the ODQO presentation is much more sensitive for extracting the localized hole states.

Following Ref. 15, we also used the ODQO technique to distinguish between the equilibrium and nonequilibrium concentration of the 2D carriers. Figure 5(b) shows the dependence of the 2DEG concentration on the light pumping (I_{pump}). The equilibrium (dark) concentration is obtained by

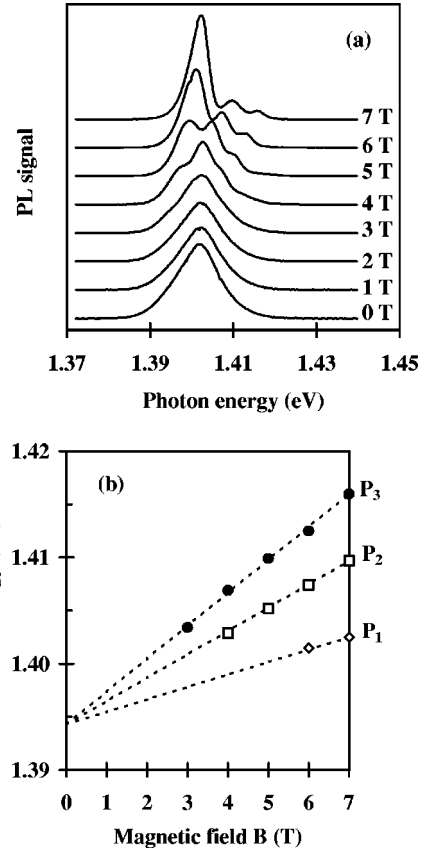


FIG. 6. (a) PL spectra from sample 2 under various magnetic fields. The strong modification of low-energy tail results from the participation of exciton recombination. (b) Landau level fan plot for sample 2. P_1 corresponds to the $0 \rightarrow 0$ transition, P_2 to the forbidden $1 \rightarrow 0$ transition, and P_3 to the $1 \rightarrow 1$ transition.

extrapolating the nonequilibrium concentration to an excitation density of zero. The point on the vertical axis shows the equilibrium 2DEG concentration derived from SdH measurements.

A similar set of experiments was carried out for our sample 2. Following our previous results,⁸ one should expect the narrowing of the PL feature with a large excitonic contribution. What we observe is a PL signature with width of about 15 meV. Using the sheet concentration $N_s = 2.5 \times 10^{11} \text{ cm}^{-2}$, the Fermi energy is calculated to lie 9 meV above the subband. The profile of the PL peak is strongly distorted due to low-energy tail at low excitation level ($< 1 \text{ W/cm}^2$). When the intensity of the exciting light reaches the value of 30 W/cm^2 , the profile becomes symmetric. The behavior in sample 2 becomes more complicated as the magnetic field and temperature increase. Figure 6(a) shows the transformation of the low-temperature PL spectrum when the magnetic field is swept from 0 up to 7 T. The high-energy side of the PL peak behaves similarly to that observed for sample 1, where the spectral peculiarities were determined by degenerate 2DEG. Figure 6(b) shows the LL fan plot from the data of Fig. 6(a) and demonstrates the presence of $0 \rightarrow 0$, $1 \rightarrow 0$, and $1 \rightarrow 1$ transitions, including both quantum-number-allowed ($\Delta N = 0$) as well as nominally forbidden ($\Delta N = 1$) transitions. The presence of the latter transitions is related to the residual disorder, which breaks the translational symmetry and thereby weakly allows

$\Delta N \neq 0$ transitions. The extrapolation to $B=0$ T gives energy gap $E_g = 1.394$ eV. The low-energy side of the PL reveals an additional peak, which strongly overlaps with the inter-LL $0 \rightarrow 0$ transition. Being shifted in energy by approximately 4 meV, it can be assigned to an exciton transition, an assignment that is also consistent with our previous data.⁸ The excitonic nature also explains the strong redistribution of the magnitudes of magnetic-field-assisted PL features. The relative magnitudes of the PL components are also dependent on temperature. The high-energy peak becomes strongly enhanced in comparison with the foregoing peak from the side of lower energy at temperature $T \gtrsim 50$ K. Unfortunately the ODQO shows only smeared peaks indicating an absence of preferable localization near the valence band.

IV. CONCLUSIONS

A magnetoluminescence study was carried out in pseudomorphic modulation-doped $\text{Al}_x\text{Ga}_{1-x}\text{As}/\text{In}_y\text{Ga}_{1-y}\text{As}/\text{GaAs}$ quantum-well structures with the QW widths less the critical

layer thickness and therefore without the generation of misfit dislocations. The data show that the structure of PL spectra in magnetic fields is determined both by the 2DEG behavior and by the presence of localized holes. The conditions for hole localization have been explored by means of optical detection of quantum oscillations via PL in a magnetic field. Using this technique, the presence of localized hole states, separated by 10 meV from the valence band, were clearly observed. This localization is assumed to be caused by alloy fluctuations, probably in In content. An alternative explanation given by Hawrylak, Pulsford, and Ploog²⁴ involves the changes in the Hartree self-consistent potential, which could also result in changes of the wave-function overlap. In this latter case, the holes could be localized in the acceptor level.

ACKNOWLEDGMENTS

The authors are indebted to A. Körle for substrate preparation. This work was supported in part by the Volkswagen Stiftung.

*Electronic address: massel@physik.hu-berlin.de

- ¹T. Ando, A. Fowler, and F. Stern, *Rev. Mod. Phys.* **54**, 437 (1982).
- ²I. V. Kukushkin and V. B. Timofeev, *Zh. Éksp. Teor. Phys.* **93**, 1088 (1987) [*Sov. Phys. JETP* **66**, 613 (1987)].
- ³R. Cingolani, W. Stolz, and K. Ploog, *Phys. Rev. B* **40**, 2950 (1989).
- ⁴B. B. Goldberg, D. Heiman, A. Pinczuk, L. Pfeiffer, and K. West, *Phys. Rev. Lett.* **65**, 641 (1990).
- ⁵T. G. Andersson, Z. G. Chen, V. D. Kulakovskii, A. Uddin, and J. T. Vallin, *Phys. Rev. B* **37**, 4032 (1988).
- ⁶L. V. Butov, V. D. Kulakovskii, T. G. Andersson, and Z. G. Chen, *Phys. Rev. B* **42**, 9472 (1990).
- ⁷S. Wang, T. G. Andersson, V. D. Kulakovskii, and J. Yao, *Superlattices Microstruct.* **9**, 123 (1991).
- ⁸H. Kissel, U. Müller, C. Walther, W. T. Masselink, Yu. I. Mazur, G. G. Tarasov, and Z. Ya. Zhuchenko, *Phys. Rev. B* **58**, 4754 (1998).
- ⁹A. Pinczuk, J. Shah, C. Miller, A. C. Gossard, and W. Wiegman, *Solid State Commun.* **50**, 735 (1984).
- ¹⁰M. S. Skolnick, J. M. Rorison, K. J. Nash, D. J. Mowbray, P. R. Tapster, S. J. Bass, and A. D. Pitt, *Phys. Rev. Lett.* **58**, 2130 (1987).
- ¹¹H. Kalt, K. Leo, R. Cingolani, and K. Ploog, *Phys. Rev. B* **40**, 12017 (1989).
- ¹²M. S. Skolnick, K. J. Nash, M. K. Saker, and S. J. Bass, *Phys. Rev. B* **50**, 11771 (1994).

- ¹³M. S. Skolnick, K. J. Nash, P. R. Tapster, D. J. Mowbray, S. J. Bass, and A. D. Pitt, *Phys. Rev. B* **35**, 5925 (1987).
- ¹⁴F. Iikawa, M. L. F. Abbade, J. A. Brum, A. A. Bernussi, R. G. Pereira, and G. Borghs, *Phys. Rev. B* **54**, 11360 (1996).
- ¹⁵I. A. Buyanova, W. M. Chen, A. V. Buyanov, W. G. Bi, and C. W. Tu, *Appl. Phys. Lett.* **69**, 809 (1996).
- ¹⁶S. K. Lyo and E. D. Jones, *Phys. Rev. B* **38**, 4113 (1988).
- ¹⁷W. Chen, M. Fritze, A. V. Nurmikko, D. Ackley, C. Colvard, and H. Lee, *Phys. Rev. Lett.* **64**, 2434 (1990).
- ¹⁸E. D. Jones, S. K. Lyo, I. J. Fritz, J. M. Klem, J. E. Schiber, C. P. Tiggers, and T. J. Drummond, *Appl. Phys. Lett.* **54**, 2227 (1989).
- ¹⁹A. R. Alves, L. A. Cury, P. S. S. Guimaraes, and M. V. B. Moreira, *Superlattices Microstruct.* **21**, 591 (1997).
- ²⁰M. S. Skolnick, P. R. Tapster, S. J. Bass, N. Apsley, A. D. Pitt, N. G. Chew, A. G. Cullis, S. P. Aldred, and C. A. Warwick, *Appl. Phys. Lett.* **48**, 1455 (1986).
- ²¹S. J. Bass, S. J. Bennett, G. T. Brown, N. G. Chew, A. G. Cullis, A. D. Pitt, and M. S. Skolnick, *J. Cryst. Growth* **79**, 378 (1986).
- ²²M. S. Skolnick, D. J. Mowbray, D. M. Whittaker, and R. S. Smith, *Phys. Rev. B* **47**, 6823 (1993).
- ²³L. V. Butov, V. I. Grinev, V. D. Kulakovskii, and T. G. Andersson, *Phys. Rev. B* **46**, 13627 (1992).
- ²⁴P. Hawrylak, N. Pulsford, and K. Ploog, *Phys. Rev. B* **46**, 15193 (1992).